Persistence in *q*-state Potts model: A mean-field approach

G. Manoj
Department of Physics and Center for Stochastic Processes in Science and Engineering, Virginia Polytechnic Institute and State University, Blacksburg, Virginia 24061
(Received 15 July 2002; published 18 February 2003)

We study the persistence properties of the $T=0$ coarsening dynamics of one-dimensional q-state Potts model using a modified mean-field approximation (MMFA). In this approximation, the spatial correlations between the interfaces separating spins with different Potts states is ignored, but the correct time dependence of the mean density $P(t)$ of persistent spins is imposed. For this model, it is known that $P(t)$ follows a power-law decay with time, $P(t)\sim t^{-\theta(q)}$, where $\theta(q)$ is the q-dependent persistence exponent. We study the spatial structure of the persistent region within the MMFA. We show that the persistent site pair correlation function $P_2(r,t)$ has the scaling form $P_2(r,t)=P(t)^2 f(r/t^{1/2})$ for all values of the persistence exponent $\theta(q)$. The scaling function has the limiting behavior $f(x)\sim x^{-2\theta}$ ($x\ll 1$) and $f(x)\to 1$ ($x\gg 1$). We then show within the independent interval approximation (IIA) that the distribution $n(k,t)$ of separation k between two consecutive persistent spins at time t has the asymptotic scaling form $n(k,t)=t^{-2\phi}g(t,k/t^{\phi})$, where the dynamical exponent has the form $\phi=\max(1/2,\theta)$. The behavior of the scaling function for large and small values of the arguments is found analytically. We find that for small separations $k\ll t^{\phi}$, $n(k,t)\sim P(t)k^{-\tau}$, where $\tau=\max[2(1-\theta),2\theta]$, while for large separations $k\gg t^{\phi}$, $g(t,x)$ decays exponentially with x. The unusual dynamical scaling form and the behavior of the scaling function is supported by numerical simulations.

DOI: 10.1103/PhysRevE.67.026115 PACS number(s): 05.50.+q, 05.40.−a, 05.45.Df, 82.20.−w

I. INTRODUCTION

In recent times, the notions of persistence and the associated persistence exponent has become one of the active topics of research in nonequilibrium physics [1]. In general, the persistence probability $P(t)$ is the probability that a stochastic variable $\phi(t)$ remains above or below a certain arbitrary value (say, its initial value) for a time interval $[0{:}t]$. The idea of persistence is particularly relevant in coarsening systems, where $P(t)$ has the natural interpretation of being the fraction of space in the system which remains in the same phase, starting from a random initial configuration. In these systems (as in some other systems also), $P(t)$ typically decays as a power law at large t, with an exponent that is nontrivial to compute and does not appear to be simply related to other known exponents that characterize the process.

The coarsening dynamics of the one-dimensional q-state Potts model at zero temperature is one of the few cases where the persistence exponent $\theta(q)$ is known exactly. The solution was provided by Derrida *et al.* through a mapping of the process to a coagulation model in steady state [2]. It was shown that at late times t, well beyond the time scale of equilibration, the fraction of persistent spins left in a finite system of linear dimension L scale as $P_q(t\gg L^2,L)\sim L^{-2\theta(q)}$, where $\theta(q)$ is given by the nontrivial expression

$$\theta(q)=-\frac{1}{8}+\frac{2}{\pi^2}\left[\cos^{-1}\left(\frac{2-q}{q\sqrt{2}}\right)\right]^2. \tag{1}$$

For times $t\ll L^2$, it follows that $P_q(t)\sim t^{-\theta(q)}$. An interesting question in this context is about the spatial distribution of spins which are persistent up to any given time t. Clearly, in a many-body process like the time evolution of Potts model, the probability that a given spin is persistent is closely linked to the state of other spins. This interdependence of spins is crucial as it makes the time evolution at any single site strongly non-Markovian, which makes the computation of the persistence exponent highly nontrivial. A study of the spatial aspects of the persistence problem is, therefore, important from the point of view of developing an intuitive understanding of the phenomenon, and also illuminates the interplay between persistence decay and the underlying domain coarsening process.

The spatial distribution of persistent sites and its time evolution have been studied previously through numerical simulations in one-dimensional (1D) diffusion equation [3], q-state Potts model [4–7], two-dimensional Ising model [8], and one-dimensional Ising model with parallel dynamics [9]. An analytic study using a rate equation approach under the independent interval approximation (IIA) has been carried out for one-dimensional $A+A\to\varnothing$ model, which is closely related to 1D Ising model [6]. It is now generally understood from physical arguments and simulations that for a coarsening process in d dimensions where the characteristic length scale has the power-law growth $L(t)\sim t^{1/z}$, the set of persistent sites forms a fractal structure with fractal dimension $d_f=d-z\theta$ over length scales $r\ll t^{1/z}$ [7,10]. The distribution is homogeneous beyond this length scale. Furthermore, since $d_f\geqslant 0$, the distribution is expected to be homogeneous over all length scales if $\theta>d/z$. This has important consequences for systems like the Potts model where θ changes with the Potts state q. In particular, for Potts model in $d=1$, Bray and O'Donoghue [7] argued that a transition from fractal to homogeneous distribution occurs as θ crosses $\frac{1}{2}$. This transition is also marked by an abrupt change in the dynamical exponent characterizing the separation between persistent sites. The characteristic length scale was conjectured to have the unusual dynamical scaling form $\mathcal{L}(t)\sim t^{\phi}$ with ϕ

$=\max(\frac{1}{2},\theta)$. This conjecture based on physical arguments was supported by numerical simulations [7].

In this paper, we use a mean-field approach to address the problem of spatial distribution of persistent sites in q-state Potts model. The essential idea behind this approach is as follows. It is well known that the $T=0$ coarsening dynamics of the q-state Potts model can be mapped to a reaction-diffusion process. In this process, the interfaces between different species of Potts spins are represented by diffusing particles A, which annihilate or coagulate upon meeting with q-dependent probabilities. In the mean-field approach, these diffusing particles are treated as homogeneously distributed, with (time dependent) density equal to the average density in the original reaction-diffusion problem. This approach has been discussed in some earlier works as a heuristic argument [11] and as a toy model for persistence [12]. We argue that this approach yields a lower bound for the persistence exponent in the Potts model. We then construct an artificial model which is devoid of spatial correlations among diffusing particles, but with persistence exponent tuned to be exactly equal to the Potts model value. We refer to this model as the modified mean-field approximation (MMFA) and use this approximation to study the spatial distribution of persistent sites in q-state Potts model.

We outline our main results at this point. Within the MMFA, we show analytically that the correlation length for the spatial distribution of persistent spins scales as $\xi(t) \sim t^{1/2}$ and the equal time pair correlation function $P_2(\mathbf{r},t)$ (defined as the probability that the spin at origin and the point $\mathbf{r}$ are persistent at time t) has the scaling form $P_2(\mathbf{r},t)=P(t)^2 f(r/\sqrt{t})$ for any value of θ. This shows that the persistent spins have a fractal distribution with $d_f=1-2\theta$ over length scales $r \ll t^{1/2}$ when $\theta<\frac{1}{2}$, but $d_f=0$ when $\theta \geqslant \frac{1}{2}$. We find that the characteristic length scale of the spatial distribution of persistent spins has the unusual scaling form $\mathcal{L}(t) \sim t^{\phi}$, where $\phi=\max(\frac{1}{2},\theta)$, in agreement with the conjecture in Ref. [7]. The empty interval distribution itself has the scaling form $n(k,t)=\mathcal{L}(t)^{-2} g[t,k/\mathcal{L}(t)]$, where $g(t,x) \sim t^{-\psi} x^{-\tau}$ for $x \ll 1$ and decays exponentially with x when $x \gg 1$. The exponents ψ and τ depends on θ through the relations $\psi=\theta(2\theta-1)H(\theta-\frac{1}{2})$ and $\tau=\max[2(1-\theta),2\theta]$, where $H(x)$ is the Heaviside step function. We support these results with numerical simulations.

The paper is arranged as follows. In the following section, we outline the mean-field approach. In Sec. III, we introduce the MMFA and compute the pair correlation and empty interval distribution of persistent sites to characterize their spatial distribution. These predictions are compared with the results of numerical simulations in the q-state Potts model in Sec. IV. We summarize our results and present our conclusions in Sec. V.

II. THE MEAN-FIELD APPROXIMATION

In the zero temperature coarsening dynamics of q-state Potts model in $d=1$, the interfacial points between different species of Potts spins perform independent random walks on the lattice and annihilate each other with probability $1/(q-1)$, or coagulate with probability $(q-2)/(q-1)$. In the process, persistent sites are "wiped out," and the surviving random walkers build up spatial correlations among themselves. The distribution of intervals between the surviving random walkers at any (sufficiently late) time t is described by a (stationary) scaling function which is known exactly for all values of q [13]. The average density $n(t)$ at time t decays as

$$n(t) \simeq \frac{q-1}{q} \frac{1}{\sqrt{2\pi t}} \tag{2}$$

asymptotically [13]. The essential idea behind the mean-field (MF) approximation is to treat the random walkers as forming a homogeneous background of average density $n(t)$, as far as the persistent sites are concerned. We define the persistence probability $P(t)$ as the probability that the site at the origin is unvisited by any walker till time t. Then, the probability that the site the probability that the site is visited by a walker between time t and $t+dt$ is $-\partial P(t)/\partial t$. Let $R(x,t)$ be the probability that the site at origin is visited by a walker for the first time at time t, whose initial position was x at $t=0$. Within the MF approximation, any walker would survive with probability $n(t)$, and the probability that it will make a first visit to origin at time t is given by $q(x,t)=\sqrt{2/\pi}(x/t^{3/2})e^{-x^2/2t}$ [14]. It follows that $R(x,t)=n(t)q(x,t)$. We now integrate $R(x,t)$ over all initial positions x and multiply by the probability that the origin is persistent at time t, which is simply $P(t)$. So we find

$$\frac{\partial P(t)}{\partial t} = -P(t)n(t)K_1(t), \quad d=1, \tag{3}$$

where $K_1(t)=\int_{-\infty}^{\infty} q(x,t)dx$ is the Smoluchowski constant [15] in $d=1$. After substituting for $q(x,t)$ and $n(t)$, we find $\partial P(t)/\partial t = -\theta^*/tP(t)$, so that $P(t) \sim t^{-\theta^*(q)}$, and $\theta^*(q)=(\sqrt{2}/\pi)(q-1)/q$ is the persistence exponent within the MF model [12]. It is interesting to compare the mean-field prediction for θ with the exact value of the exponent. For $q=2$, $\theta^*(2) \simeq 0.225$, while the exact value from Eq. (1) is $\frac{3}{8}$. For the $q=\infty$ case, the MF model predicts $\theta^*(\infty) \simeq 0.45$, which is to be compared with the exact value $\theta(\infty)=1$. Upon extending the comparison to the entire range of values of q, it is clear that the mean-field treatment consistently underestimates the value of θ.

We now argue that $\theta^*(q)$ is, in fact, a lower bound for $\theta(q)$. In the mean-field approach discussed so far, it is assumed that the random walkers disappear from the lattice at random at such a rate so that their average density falls as $n(t)$. The actual reaction-diffusion process is quite different, because only walkers which come very close to another walker are likely to be removed. Clearly in regions of space where walkers come close to each other, they are likely to visit the same site again and again. This effect is much more within the mean-field approach, where the walkers actually pass through each other, possibly several times before disappearing. Thus, it is plausible that for the same average density of walkers, a larger number of persistent sites will be

visited in the actual reaction-diffusion model, compared to its mean-field analogue. Since this is true for all times, the average density of persistent sites in mean-field theory will be higher than the same in the actual Potts model dynamics. This would naturally imply that

$$\theta^*(q) \leqslant \theta(q). \tag{4}$$

Interestingly, we show now that the mean-field argument presented above yields the correct value for the persistence exponent for $A+A \rightarrow \varnothing$ model in $d=2$. This is not surprising, since for this model, the upper critical dimension is $d_c=2$, and the mean-field treatment becomes exact above this dimension. It can be shown that in $d=2$, the probability that a random walker starting at an an arbitrary point crosses a circle of radius a around the origin for the first time at t is given by the expression [16]

$$K_2(t) \simeq \frac{4\pi D}{\log(4Dt/a^2)}, \quad t \gg a^2/D, \tag{5}$$

which is the analogue of Smoluchowski constant in $d=2$. The asymptotic particle density decay for $A+A \rightarrow \varnothing$ model in $d=2$ has the form $n(t) \simeq (1/8\pi)[\log(Dt)/Dt]$ [17]. Upon extending the MF arguments presented previously, we find that

$$\frac{\partial P(t)}{\partial t} = -P(t)n(t)K_2(t), \quad d=2, \tag{6}$$

After substituting for $n(t)$ and $K_2(t)$, and taking the limit $a \rightarrow 0$, we find that $P(t) \sim t^{-1/2}$ so that $\theta^*=1/2$ in $d=2$. This result is exact, as has been shown by a rigorous field-theoretic calculation [11].

We thus observe that while the mean-field approach, in general, gives only a lower bound for the persistence exponent, it correctly identifies the essential features that brings about this power-law decay, i.e., the diffusive motion of interfacial points and the $1/\sqrt{t}$ decay in their overall density. In the following sections, we use a slightly modified version of this treatment to study the spatial distribution of persistent sites in q-state Potts model.

III. THE MODIFIED MEAN-FIELD APPROXIMATION

Our purpose is to use the mean-field approach to study the spatial distribution of persistent spins in the q-state Potts model, and in particular, to understand the transition from fractal to homogeneous distribution as θ crosses $\frac{1}{2}$. However, it may be noted that in the mean-field approximation to the dynamics of the Potts model, the largest value of θ (attained at $q=\infty$) is $2/\sqrt{\pi} \simeq 0.45$ which is less than the transition value $\frac{1}{2}$. This problem is circumvented by defining an artificial model where we define the diffusing particles as noninteracting random walkers, who can pass through each other. The model also allows for multiple occupancy of lattice sites. The dynamics consists of random walkers being picked at random and taken out of the lattice at a time-dependent rate, which is tuned to produce power-law decay $P(t) \sim t^{-\theta'}$ with any arbitrary θ'. From the arguments presented in the preceding section, it is obvious that this would be the case if the average density were to decay as $n(t) \sim \sqrt{\pi/2}(\theta'/\sqrt{t})$ asymptotically. By construction, this model is devoid of spatial correlations among reacting particles (i.e., it is still mean-field) but θ' is now arbitrary. If we now choose $\theta'=\theta(q)$, this model is an approximation to the q-state Potts model, with the simplifying feature that the spatial correlation between interfacial points is now absent. We shall refer to this model as the MMFA for the original Potts model.

A. Pair correlation for persistent spins within the MMFA

In this section, we compute the equal time pair correlation function for persistent spins in q-state Potts model under the MMFA. We define $P_2(r,t)$ as the probability that both the site at origin and the site at $r>0$ are persistent at time t. Our purpose is to compute $P_2(r,t)$ for various r.

The generalization of Eq. (3) to this case is

$$-\frac{\partial P_2(r,t)}{\partial t} = 2P_2(r,t)\int_{-\infty}^{r} R_r(x,t)\,dx, \tag{7}$$

where $R_r(x,t)$ is the probability that a particle with initial position $x(-\infty<x<r)$ will make a first visit to the origin at time t, *without ever crossing* r in the interval [0:t]. The factor 2 in front takes into account the probability that either of the sites could be reached by one of the diffusing particles. Unlike the first case, $R_r(x,t)$ is now different for $x<0$ and $0 \leqslant x<r$. For $x<0$, the constraint of no crossing at r is irrelevant for the computation of $R_r(x,t)$, since to reach r, the particle would have to cross the origin first. So $R_r(x,t)=R(x,t)$ simply for $x<0$, and so

$$\int_{-\infty}^{0} R_r(x,t)\,dx = \frac{\theta}{2t}. \tag{8}$$

For $x>0$, this is no longer true, and $R_r(x,t)$ needs to be computed separately. The quantity that we need here is $q_r(x,t)$, the probability that a diffusing particle whose position at $t=0$ is x, will reach the origin for the first time at t, without ever crossing the point r in between. Then $R_r(x,t)=n(t)q_r(x,t)$. To find $q_r(x,t)$, let us use the following standard method. Consider a random walk starting from $0<x<r$ at $t=0$ with absorbing barriers at 0 and r. If the probability distribution of the position z of the walker at time t is $u_x(z,t)$, then

$$q_r(x,t) = \left.\frac{\partial u_x(z,t)}{\partial z}\right|_{z=0}. \tag{9}$$

The expression for $u_x(z,t)$ is known exactly, and the asymptotic form at large t [14] is

$$u_x(z,t) = \frac{1}{\sqrt{2\pi t}} \sum_{k=-\infty}^{\infty} e^{-(z-x-2kr)^2/2t} - e^{-(z+x-2kr)^2/2t} \tag{10}$$

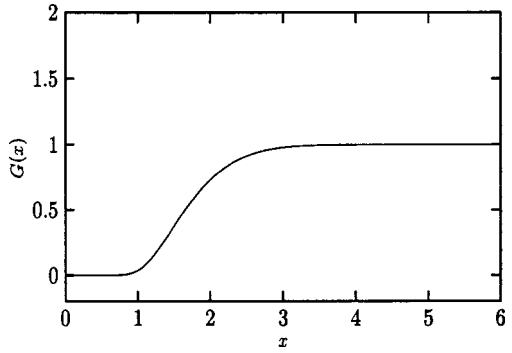

FIG. 1. Plot of $G(x)$ vs x.

from which, we find

$$q_r(x,t)=\frac{1}{\sqrt{2\pi t}}\sum_{k=-\infty}^{\infty}\frac{x+2kr}{t}e^{-(z-x-2kr)^2/2t} - \frac{x-2kr}{t}e^{-(z+x-2kr)^2/2t}. \quad (11)$$

We note that for $r\gg t^{1/2}$, the $k=0$ mode is the dominant term in the sum, and this gives $q_r(x,t)\approx\sqrt{2/\pi t^3}xe^{-x^2/2t}$ + smaller terms that vanish as $(r/t^{1/2})\to\infty$. Clearly in this limit, we recover the $r=\infty$ term, as we should. It then follows that

$$\int_0^r R_r(x,t)dx=\frac{\theta}{2t}G\left(\frac{r}{\sqrt{t}}\right), \quad (12)$$

where

$$G(x)=1-\eta+\sum_{k=1}^{\infty}2\eta^{4k^2}-\eta^{(1+2k)^2}-\eta^{(1-2k)^2}, \quad (13)$$

with $\eta=e^{-x^2/2}$. After substitution of Eq. (8) and Eq. (12) in Eq. (7), we find

$$\frac{\partial P_2(r,t)}{\partial t}=-2P_2(r,t)\frac{\theta}{2t}\left[1+G\left(\frac{r}{\sqrt{t}}\right)\right], \quad (14)$$

which admits a scaling solution of the form

$$P_2(r,t)=P(t)^2 f\left(\frac{r}{\sqrt{t}}\right), \quad (15)$$

and the scaling function $f(x)$ is given by the following expression:

$$\frac{x}{2}\frac{\partial f}{\partial x}=-\theta f(x)[1-G(x)]. \quad (16)$$

Let us now consider the limiting behavior of the scaling function for $x\ll 1$ and $x\gg 1$. In the first case, it is clear from Fig. 1 that $G(x)\approx 0$, and so $(x/2)(\partial f/\partial x)=-\theta f(x)$, which implies that $f(x)\sim x^{-2\theta}$ as $x\to 0$. In the opposite extreme $G(x)\to 1$ as $x\to\infty$, and so $(x/2)(\partial f/\partial x)\approx 0$, which means that $f(x)$ approaches a constant value in this limit. It is further clear that, from the definition of the scaling function as given by the Eq. (15), this constant is unity, since we expect $P_2(r,t)\to P(t)^2$ as $r\to\infty$. For convenience of later calculations, we approximate the scaling function as

$$f(x)=\begin{cases}a^{2\theta}x^{-2\theta}, & x\leqslant a\\ 1, & x>a,\end{cases} \quad (17)$$

where a is a number, of order unity.

We see that under the MMFA, the pair correlation function has a scaling form which is same for all values of θ, with power-law decay $P_2(r,t)\sim P(t)r^{-2\theta}$ for short distances $r\ll t^{1/2}$. As is well known, power-law decay of pair correlation function points to the underlying scale invariance of the spatial distribution of the persistent spins. This is characteristic of a fractal distribution under some circumstances. To see this, let us first define $C(r,t)=P(t)^{-1}P_2(r,t)$, which is the probability of finding a persistent spin at a distance r from another persistent spin. Now, the integral $M(R,t)=\int_1^R C(r,t)dr$ is the total number of persistent spins within a radius R of a persistent spin. Clearly, from the scaling form described above, $M(R,t)\sim R^{d_f}$ for $R\ll t^{1/2}$, where $d_f=\max(1-2\theta,0)$. For $R\gg t^{1/2}$, we find that $M(R,t)\simeq RP(t)$, which is simply a homogeneous distribution. Thus, if we look at length scales $R\ll t^{1/2}$, there is a fractal structure when $\theta<\frac{1}{2}$. However, when $\theta\geqslant\frac{1}{2}$, this scale-invariant structure is replaced by a few isolated sites, whose number does not grow with the length scale of observation.

Clearly, the spatial distribution of persistent spins undergoes a transition as θ crosses $\frac{1}{2}$. Indeed, if we consider time scales beyond equilibration time $t\gg L^2$, for $\theta<\frac{1}{2}$ the total number of persistent spins left in the system scales as $L^{1-2\theta}$, whereas for $\theta\geqslant\frac{1}{2}$, there are only a finite number of persistent spins left. This important difference is not adequately reflected in the pair correlation function, which has the same scaling form for all values of θ. In the following section, we study another quantity to characterize the spatial distribution which undergoes a rather significant change in its scaling properties across the transition. This quantity is the empty interval distribution, which is one of the standard tools in the study of one-dimensional reaction-diffusion processes.

B. The empty interval distribution

An empty interval, in our convention, is the separation between two consecutive persistent sites. The empty interval distribution (EID) $n(k,t)$ is defined as the number of such intervals of length k at time t. For convenience, we also divide this quantity with the system size N so that $n(k,t)$ satisfies the following normalization conditions:

$$\int_1^\infty n(k,t)dk=P(t), \qquad \int_1^\infty kn(k,t)dk=1. \quad (18)$$

Computing the EID directly, even under the mean-field approximation, is nontrivial. Instead, we shall compute it from the pair correlation function using the IIA, where the lengths of successive empty intervals are considered as inde-

pendent random variables. The IIA has been a valuable tool in the study of one-dimensional problems, and has been successfully applied to study spatial distribution of persistent spins in $A+A\rightarrow\varnothing$ model. Under the IIA, the relation between $n(k,t)$ and $P_2(r,t)$ is

$$P_2(r,t)=n(r,t)+P(t)^{-1}\int_1^r dx\, n(x,t)P_2(r-x,t). \tag{19}$$

It is convenient to express this relation in terms of the Laplace transforms $\tilde{C}(p,t)=\int_1^\infty C(r,t)e^{-pr}dr$ and $\tilde{n}(p,t)=\int_1^\infty n(s,t)e^{-ps}ds$, where $C(r,t)$ was defined in the preceding section. Under these transformations, Eq. (19) maybe expressed in the form

$$\tilde{n}(p,t)=\frac{P(t)\tilde{C}(p,t)}{1+\tilde{C}(p,t)}. \tag{20}$$

From the scaling form for $P_2(r,t)$ given by Eq. (15), we find that

$$\tilde{C}(p,t)=P(t)\sqrt{t}I(q,t), \tag{21}$$

where $q=p\sqrt{t}$, and $I(q,t)=\int_{t^{-1/2}}^\infty f(x)e^{-qx}dx$ The lower limit is put as $t^{-1/2}$ instead of zero to take care of possible small argument divergence in the scaling function.

Let us first consider the case, where $\theta<\frac{1}{2}$: In this case the scaling function $f(x)$ is integrable, so we put the lower limit in the previous equation as zero. Using Eq. (17), we find that

$$I(q,t)=a^{2\theta}q^{2\theta-1}\gamma(1-2\theta,qa)+\frac{1}{q}e^{-qa},\quad \theta<\frac{1}{2}, \tag{22}$$

where $\gamma(\alpha,x)=\int_0^x e^{-t}t^{\alpha-1}dt$ is the incomplete γ function. After substituting in Eq. (20) and Eq. (21), and taking the $t\rightarrow\infty$ limit (keeping q fixed), we find

$$\tilde{n}(p,t)=t^{-1/2}\left[P(t)t^{1/2}-\frac{q}{a^{2\theta}q^{2\theta}\gamma(1-2\theta,qa)+e^{-qa}}\right]. \tag{23}$$

It follows that

$$n(k,t)=t^{-1}h\left(\frac{k}{t^{1/2}}\right), \tag{24}$$

so that

$$\tilde{n}(p,t)=t^{-1/2}[t^{1/2}P(t)-h_1(q)], \tag{25}$$

which has the same form as Eq. (23), and $h_1(q)=\int_0^\infty h(x)[1-e^{-qx}]dx$. After integrating by parts, we find

$$h_1(q)=-G(\infty)+q[\lim_{x\rightarrow 0}xG(x)+\tilde{G}(q)], \tag{26}$$

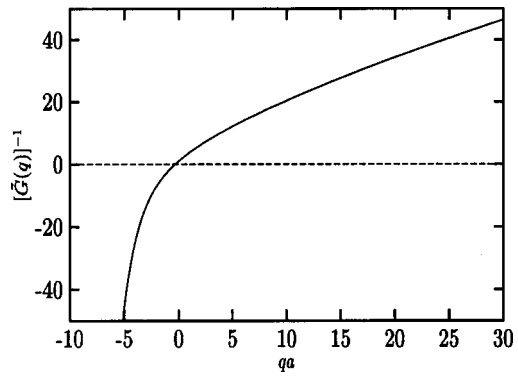

FIG. 2. The figure shows the inverse of $\tilde{G}(q)$ plotted against qa.

where $G(x)=\int_x^\infty h(y)dy$ and $\tilde{G}(q)=\int_0^\infty G(x)e^{-qx}dx$. We assume that $G(x)$ is integrable, so that $\lim_{x\rightarrow 0}xG(x)=0$ and $G(\infty)=0$. Finally, we have

$$\tilde{G}(q)=\frac{1}{a^{2\theta}q^{2\theta}\gamma(1-2\theta,qa)+e^{-qa}}. \tag{27}$$

Now we may try to deduce the behavior of the function $G(x)$ at large and small arguments from its Laplace transform(LT) given by the previous equation. To find the behavior of $G(x)$ near $x=0$, we use the standard formula [18]

$$\lim_{t\rightarrow 0}t^{-\rho}g(t)=\lim_{s\rightarrow\infty}\frac{s^{\rho+1}\tilde{g}(s)}{\rho!},\quad \rho>-1, \tag{28}$$

where $\tilde{g}(s)$ is the LT of $g(t)$. Now, for large q, $\gamma(1-2\theta,qa)\simeq\Gamma(1-2\theta)$, so that $\tilde{G}(q)=a^{-2\theta}q^{-2\theta}/\Gamma(1-2\theta)$ as $q\rightarrow\infty$. It follows that $\lim_{x\rightarrow 0}x^{1-2\theta}G(x)=a^{-2\theta}/(2\theta-1)!\Gamma(1-2\theta)$ from which we find

$$G(x)\sim\frac{a^{-2\theta}x^{2\theta-1}}{(2\theta-1)!\Gamma(1-2\theta)},\quad x\rightarrow 0 \tag{29}$$

and, after using the relation $h(x)=-\partial G/\partial x$,

$$h(x)\sim x^{-2(1-\theta)},\quad x\rightarrow 0. \tag{30}$$

The behavior of $G(x)$ at large x, one has to look for the singularities of $\tilde{G}(q)$ in Eq. (27). If $\tilde{G}(q)$ has a singularity of the form $\tilde{G}(q)\sim(q-q^*)^{-\nu}$, then upon inversion of the LT, it follows that $G(x)\sim x^{\nu-1}e^{q^*x}$ as $x\rightarrow\infty$ [18]. In order to find the singularity, we plotted the denominator of Eq. (27) against its argument (Fig. 2). We find that the function crosses zero at one point in the negative q axis. By careful numerical analysis using bisection method, we have determined this crossing point to be at $q^*a=-\lambda$, where the numerical constant $\lambda\simeq 0.32$ for $\theta=\frac{3}{8}$ and $\lambda\simeq 0.85$ for $\theta=\frac{1}{2}$. This implies that the leading term in the decay of $G(x)$ at large x is exponential, i.e., $G(x)\sim\exp(-[\lambda/a]x)$ as $x\rightarrow\infty$,

with a possible power-law prefactor. Consequently, the scaling function $h(x)$ also has similar exponential decay at large x.

$$h(x)\sim e^{(\lambda/a)x}, \quad x\gg 1. \tag{31}$$

We also determine the characteristic length scales of the distribution using the scaling form for $n(k,t)$. These may be defined as the ratios of moments of the distribution.

$$L_m(t)=I_m(t)/I_{m-1}(t), \quad m=0,1,2,\ldots, \tag{32}$$

where $I_m(t)=\Sigma_k n(k,t)k^m$ are the moments of $n(k,t)$. Clearly, $L_1(t)=P(t)^{-1}\sim t^{\theta}$ by definition, whereas all higher order length scales

$$L_j(t)\sim t^{1/2}, \quad j>1, \tag{33}$$

which follows from the dynamic scaling form given by Eqs. (24), (30), and (31) for $n(k,t)$.

We now continue our study of empty interval distribution for the case, where $\theta\geqslant\frac{1}{2}$. Although the MMFA allows us to study arbitrarily large values of θ, we restrict ourselves to the regime $\theta<1$, since our basic aim is to study the persistence in q-state Potts model, where $\theta(q)\leqslant 1$. Furthermore, for $q=\infty$ where $\theta=1$, $n(k,t)$ can be found exactly [7] and is known to be a pure exponential.

For $\frac{1}{2}<\theta<1$, the scaling function $f(x)$ has a nonintegrable $x^{-2\theta}$ singularity near $x=0$ (we do not study explicitly the logarithmic singularity occurring for $\theta=\frac{1}{2}$). We integrate by parts and find

$$I(q,t)=\frac{a^{2\theta}}{2\theta-1}[t^{\theta-1/2}e^{-qt^{-1/2}}-a^{1-2\theta}e^{-qa}-q^{2\theta-1} \times\gamma(2-2\theta,qa)]+\frac{1}{q}e^{-qa}, \quad \theta\geqslant\frac{1}{2}. \tag{34}$$

Let us now define $\lambda=p/P(t)=qt^{-1/2}P(t)^{-1}$. For $t\to\infty$ and finite λ, we have

$$I(q,t)=\frac{a^{2\theta}}{2\theta-1}t^{\theta-1/2}+\frac{1}{\lambda t^{1/2}P(t)}. \tag{35}$$

After substitution in Eq. (21) we find

$$\tilde{C}(p,t)=P(t)\left[\frac{a^{2\theta}}{2\theta-1}t^{\theta}+\frac{1}{\lambda P(t)}\right]. \tag{36}$$

We define the constant $\beta=t^{\theta}P(t)a^{2\theta}/2\theta-1$, in terms of which $\tilde{C}(p,t)=\beta+1/\lambda$. Now we substitute in Eq. (20) and find

$$\tilde{n}(p,t)=P(t)\frac{\beta}{1+\beta}\left[\frac{\lambda+\beta^{-1}}{\lambda+(1+\beta)^{-1}}\right]. \tag{37}$$

Upon inversion of the LT, we find that

$$n(k,t)=P(t)^2\phi[kP(t)], \tag{38}$$

where

$$\phi(x)=\frac{\beta}{1+\beta}\left[\delta(x)+\frac{1}{\beta(1+\beta)}e^{-x(1+\beta)^{-1}}\right]. \tag{39}$$

The scaling function has a rather unnatural δ-function singularity at the origin. However, a more careful analysis show that for any finite (but still large) time t, the divergence at origin is only power-law, but with a different exponent than the previous case ($\theta<\frac{1}{2}$). We start with the expression given by Eq. (21) and Eq. (34) for $\tilde{C}(p,t)$. After keeping the leading finite t correction, we find that

$$\tilde{C}(p,t)=\beta+\frac{1}{\lambda}-\beta t^{-\theta(2\theta-1)}\lambda^{2\theta-1}. \tag{40}$$

For purposes that will be clear later, let us define $m(k,t)=kn(k,t)$ so that $\Sigma_k m(k,t)=1$. We also define the associated Laplace transform $\tilde{m}(p,t)$. The Laplace transforms are related through

$$\tilde{m}(p,t)=-\frac{\partial\tilde{n}(p,t)}{\partial p}. \tag{41}$$

Using the expression Eq. (20) for $\tilde{n}(p,t)$, we find that

$$\tilde{m}(p,t)=-\frac{P(t)\tilde{C}'(p,t)}{[1+\tilde{C}(p,t)]^2}, \tag{42}$$

where $\tilde{C}'(p,t)=\partial\tilde{C}(p,t)/\partial p$, and is given by the expression

$$\tilde{C}'(p,t)=-\frac{1}{P(t)}\left[\frac{1}{\lambda^2}+(2\theta-1)\beta t^{-\theta(2\theta-1)}\lambda^{2(\theta-1)}\right]. \tag{43}$$

After substitution in Eq. (42) and taking the limit $t\to\infty$, we find

$$\tilde{m}(p,t)=\frac{1+(2\theta-1)\beta t^{-\theta(2\theta-1)}\lambda^{2\theta}}{[1+\lambda(1+\beta)]^2}, \tag{44}$$

which gives the scaling forms

$$m(k,t)=P(t)\psi[t,kP(t)], \quad n(k,t)=P(t)^2\Phi[t,kP(t)], \tag{45}$$

where

$$x\Phi(t,x)=\psi(t,x) \tag{46}$$

by definition. The Laplace transform of the scaling function $\psi(t,x)$ is

$$\tilde{\psi}(t,\lambda)=\frac{1+(2\theta-1)\beta t^{-\theta(2\theta-1)}\lambda^{2\theta}}{[1+\lambda(1+\beta)]^2}. \tag{47}$$

We notice that if the finite t correction term is not included, $\lim_{\lambda\to\infty}\lambda^2\tilde{\psi}(t,\lambda)$ is finite, and in that case, the small

argument divergence of $\psi(t,x)$ will be sharper than any power law. This is what is reflected in the appearance of the δ function in Eq. (41). However, when this term is included, the multiplying factor has to be $\lambda^{2-2\theta}$ in order to make the resulting expression finite as $\lambda \to \infty$. This implies that the small x divergence for $\psi(t,x)$ has the power-law form $\psi(t,x) \sim t^{-\theta(2\theta-1)} x^{1-2\theta}$ for small x. From Eq. (48), we find a similar power-law divergence in $\Phi(t,x)$ also,

$$\Phi(t,x) \sim t^{-\theta(2\theta-1)} x^{-2\theta}, \quad x \ll 1. \tag{48}$$

In the large x limit, $\Phi(t,x)$ becomes time independent, and decays exponentially with x as in Eq. (39), i.e.,

$$\Phi(t,x) \simeq \frac{1}{(1+\beta)^2} e^{-x/1+\beta}, \quad x \gg 1. \tag{49}$$

The characteristic length scales are easy to compute. From the scaling form, it follows that all the characteristic lengths have identical asymptotic scaling behavior,

$$L_j(t) \sim t^{\theta}, \quad j = 1,2, \ldots . \tag{50}$$

The difference in the asymptotic scaling behavior of the characteristic length scale as θ crosses $\frac{1}{2}$ may be seen as a competition between two length scales, the diffusive length scale $\mathcal{L}_D(t) \sim \sqrt{Dt}$ which gives the mean separation between two random walkers, and the persistence scale $\mathcal{L}_p(t) = P(t)^{-1} \sim t^{\theta}$ which is the mean separation between two persistent spins. The characteristic length scale is dominated by the larger of the two, i.e., we may write

$$\mathcal{L}(t) \sim t^{\phi}, \quad \phi = \max\left(\frac{1}{2}, \theta\right), \tag{51}$$

where $\mathcal{L}(t)$ is defined through the dynamical scaling form for $n(k,t)$,

$$n(k,t) = \mathcal{L}(t)^{-2} g\left(t, \frac{k}{\mathcal{L}(t)}\right). \tag{52}$$

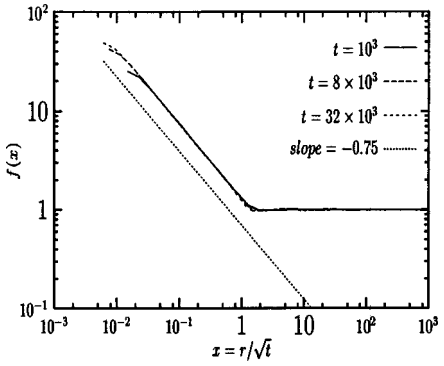

FIG. 3. The scaled pair correlation $f(x) = P(t)^{-2} P_2(r,t)$ is plotted against the dimensionless scaling variable $x = r/\sqrt{t}$ for $q = 2$ on a logarithmic scale. The straight line is a guide to eye, and has slope $2\theta(2) = 0.75$, which is the MMFA prediction. The time t is measured in MC steps and distance r is measured in units of lattice spacing.

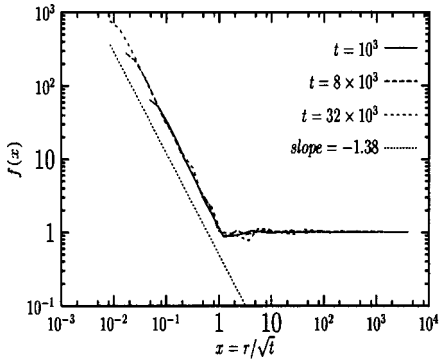

FIG. 4. Same as Fig. 3 for $q = 5$. The slope of the straight line is $2\theta(5) \simeq 1.38$, which is the MMFA prediction.

The scaling function $g(t,x) = h(x)$ when $\theta < \frac{1}{2}$ and $g(t,x) = \Phi(t,x)$ when $\theta \geq \frac{1}{2}$. In general, the small argument behavior of $g(t,x)$ has the power-law form

$$g(t,x) \sim t^{-\psi} x^{-\tau}, \quad x \to 0, \tag{53}$$

where the exponents ψ and τ are given by

$$\psi = \theta(2\theta-1) H\left(\theta - \frac{1}{2}\right), \quad \tau = \max[2\theta, 2(1-\theta)], \tag{54}$$

and $H(x)$ is the Heaviside step function. For large x, the scaling function is time independent and decays exponentially with x. We also note from the scaling form that over small distances $k \ll t^{\phi}$,

$$n(k,t) \sim P(t) k^{-\tau}, \quad k \ll t^{\phi}, \tag{55}$$

where τ is given by Eq. (54).

IV. NUMERICAL RESULTS

We studied the quantities $P_2(r,t)$ and $n(k,t)$ numerically by simulating the kinetics of q-state Potts model with random initial conditions. The time evolution of spin configurations via Glauber dynamics is implemented using the mapping of this dynamics to a reaction-diffusion problem, as mentioned in the Introduction. In this procedure, a set of

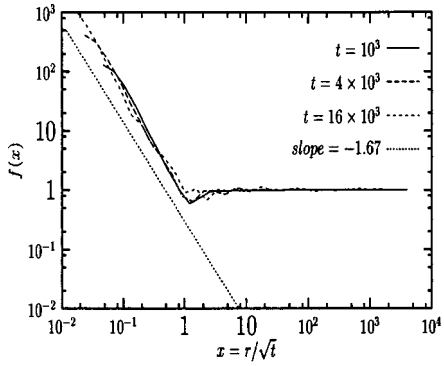

FIG. 5. Same as Fig. 3 for $q = 10$. The slope of the straight line is $2\theta(10) \simeq 1.67$, which is the MMFA prediction.

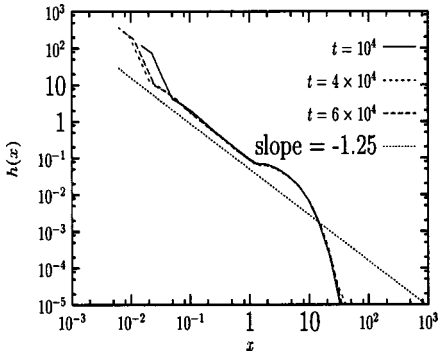

FIG. 6. The scaled EID $h(x)=tn(k,t)$ is plotted against the dimensionless scaled separation $x=k/\sqrt{t}$ for $q=2$ Potts model. The excellent scaling collapse validates the scaling form given in Eq. (24). The straight line has slope $\tau=2[1-\theta(2)]=5/4$, which is the MMFA-IIA prediction. The time t is measured in MC steps and distance k is measured in units of lattice spacing.

diffusing particles A are initially distributed at random on the lattice with a certain average initial density n_0 (which we fix as $\frac{1}{2}$). When two diffusing particles meet, they annihilate each other or coagulate with probability $1/q-1$ and $q-2/q-1$, respectively. We count one Monte Carlo (MC) step in the simulation after the position of every particle in the lattice has been updated once. Persistent spins (sites) at any time t are those sites which have not been touched by a random walker till that time. All the simulations were done on a lattice with 2^{17} sites, and the results were averaged over 100 different starting configurations. In order to check the different dynamic scaling behavior for $\theta<\frac{1}{2}$ and $\theta\geqslant\frac{1}{2}$, we did our simulations for three different values of $q=2,5$, and 10. For later reference, we note that from Eq. (1), the corresponding values of the persistence exponent are $\theta(2)=3/8=0.375, \theta(5)\approx 0.6928$, and $\theta(10)\approx 0.8310$. In Figs. 3–5, and later in Figs. 6–9, we have employed logarithmic binning of the data in intervals of size 1.5^n $(n=1,2,\ldots)$ since the statistical noise was considerable. However, for all exponent measurements, we have used only the bare(not binned) data.

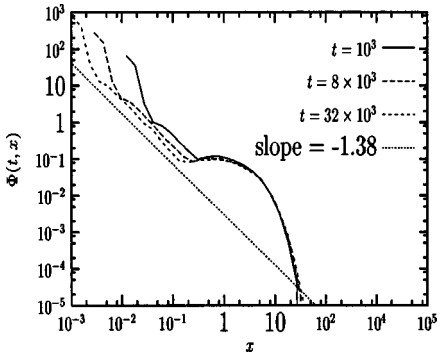

FIG. 7. The scaled EID $\Phi(t,x)=tn(k,t)$ is plotted against the scaled separation $x=kP(t)$ on a logarithmic scale for $q=5$ Potts model. We see that the scaling function is explicitly time dependent for small k, but is time independent for large k. The straight line in the figure gives the theoretical prediction $\tau=2\theta(5)\simeq 1.38$ for power-law decay at small x (see discussion in text). The time t is measured in MC steps and distance k is measured in units of lattice spacing.

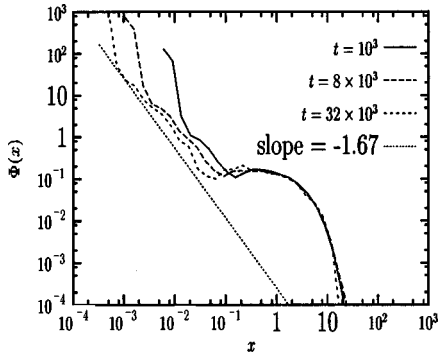

FIG. 8. Same as Fig. 10 for $q=10$. The straight line in the figure gives the theoretical prediction $\tau=2\theta(10)\simeq 1.67$ for power-law decay at small x (see discussion in text). The time t is measured in MC steps and distance k is measured in units of lattice spacing.

In Figs. 3–5, we have plotted the scaling function $f(x)$ for the pair correlation function $P_2(r,t)$ against the scaling variable $r/\sqrt{t}$ for three q values, $q=2,5$, and 10. We find excellent scaling collapse for all three values of q, which is in agreement with the dynamic scaling picture provided by the MMFA in Eq. (15). In the figures, we find power-law decay of $f(x)$ for small x, with a sharp crossover to the flat long-distance behavior, which is also in agreement with the assumption we made in Eq. (17). We also note that the constant a introduced in Eq. (17) is in fact very close to one.

In Fig. 10, we plot the characteristic length scale $L_2(t)$ against time t for $q=2,5$ and 10 and measure the dynamical exponent ϕ. The observed slopes of the lines are systematically higher than the theoretical prediction in Eq. (53) by around 0.05, while the statistical error in all the three cases was only $\sim 10^{-4}$ or smaller. The observed deviation could be possibly due to the fact that the asymptotic behavior is not fully reflected over the time scales which we used. The number of persistent spins left in the system falls rapidly with time for high values of q, and so we were forced to restrict

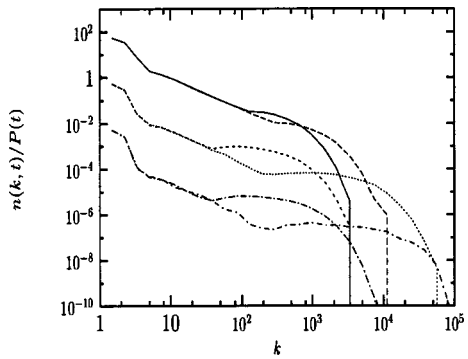

FIG. 9. In the figure, $n(k,t)/P(t)$ is plotted against k for two widely separated values of t for each value of $q=2,5$, and 10 (top to bottom). In all the cases, the function is independent of t for $k \ll t^{\phi}$, and shows the power-law decay $\sim k^{-\tau}$. We measure $\tau \simeq 1.32\pm 0.03$, 1.41 ± 0.04, and 1.61 ± 0.22 for $q=2$, $q=5$, and $q=10$, respectively. The corresponding MMFA-IIA predictions are, to the same accuracy, 1.25, 1.38, and 1.66.

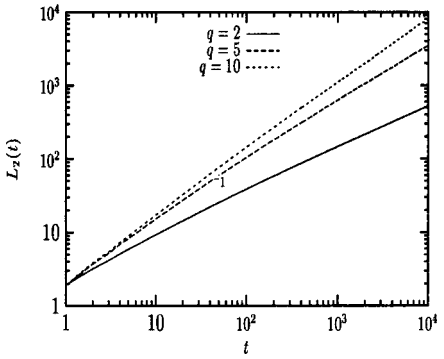

FIG. 10. The figure shows the characteristic length scale $L_2(t)$ (measured in units of lattice spacing, definition in text) plotted against time t (measured as number of MC steps) on a logarithmic scale for three Potts values $q=2$, 5, and 10. The measured slopes of the lines are, respectively, 0.5507, 0.7391, and 0.8672. The corresponding theoretical predictions are, to the same accuracy, 0.5000, 0.6928, and 0.8310.

ourselves to times $t \leqslant 32\,000$. In fact, even for $q=2$ case, previous simulations over longer time scales have shown the presence of an additive power-law correction to the asymptotic scaling behavior [6].

In Figs. 6–8, we check the dynamic scaling form Eq. (54) for $n(k,t)$ against the scaling variable $x=k/t^{\phi}$ for three values of $q=2,5$, and 10. We find that for $q=2$, excellent scaling collapse is obtained with $\phi=\frac{1}{2}$ (Fig. 6). For small x, we find power-law decay of the scaling function, which crosses over to fast exponential decay at large x. For higher values of q [where $\theta(q)>\frac{1}{2}$], we find that with $\phi=\theta$, we find very good scaling collapse for $x \gg 1$. But for $x \ll 1$, we find systematic deviation from scaling collapse, which was also observed earlier by Bray and O'Donoghue [7]. This observation supports the theoretical prediction based on MMFA, and shows that in this regime, the scaling function has explicit time dependence. To show this more clearly, and to verify the predicted time dependence, we plotted the quantity $n(k,t)/P(t)$ against k for three widely spaced values of t for all three q values studied in Fig. 8. We see that in all three cases, a simple power-law decay with k is observed for $k \ll t^{\phi}$, thus validating Eq. (55). The measurement of the exponent τ gives values in reasonable agreement with theoretical prediction, although for $q=10$, the statistical error is significant.

V. CONCLUSIONS

In this paper we have studied the spatial aspects of persistence in one dimensional q-state Potts model using a mean-field approximation. We have computed the pair correlation function for persistent spins under this approximation, and used it to compute the empty interval distribution under the independent interval approximation. We find dynamical scaling behavior in both these quantities. The time dependence of the characteristic length scale and the behavior of the scaling function was found in both cases. We showed analytically within the mean-field approximation the transition from fractal to homogeneous distribution of persistent spins as the persistence exponent crosses $\frac{1}{2}$. We support our results by numerical simulations in the kinetic q-state Potts model.

ACKNOWLEDGMENTS

This research was supported in part by Grant No. (DMR 0088451) from the U.S National Science Foundation. The author would like to thank P. Ray for a critical reading of the manuscript and suggestions for improvement.

[1] For a review, S.N. Majumdar, Curr. Sci. **77**, 370 (1999).
[2] B. Derrida, V. Hakim, and V. Pasquier, Phys. Rev. Lett. **75**, 751 (1995); J. Stat. Phys. **85**, 763 (1996).
[3] D.H. Zanette, Phys. Rev. E **55**, 2462 (1997).
[4] G. Manoj and P. Ray, e-print cond-mat/9901130.
[5] G. Manoj and P. Ray, J. Phys. A **33**, L109 (2000).
[6] G. Manoj and P. Ray, J. Phys. A **33**, 5489 (2000).
[7] A.J. Bray and S.J. O'Donoghue, Phys. Rev. E **62**, 3366 (2000).
[8] S. Jain and H. Flynn, J. Phys. A **33**, 8383 (2000).
[9] G.I. Menon, P. Ray, and P. Shukla, Phys. Rev. E **64**, 046102 (2001).
[10] G. Manoj and P. Ray, Phys. Rev. E **62**, 7755 (2000).
[11] J. Cardy, J. Phys. A **28**, L19 (1995).
[12] S.J. O'Donoghue and A.J. Bray, Phys. Rev. E **64**, 041105 (2001).
[13] B. Derrida and R. Zeitak, Phys. Rev. E **54**, 2513 (1996).
[14] W. Feller, *Introduction to Probability Theory and Applications* (Wiley, New York, 1966), Vol. 1.
[15] M. von Smoluchowski, Z. Phys. Chem., Stoechiom. Verwandtschaftsl. **92**, 129 (1917).
[16] D.C. Torney and H.M. McConnell, Proc. R. Soc. London, Ser. A **387**, 147 (1983).
[17] B.P. Lee, J. Phys. A **27**, 2633 (1994).
[18] M.G. Smith, *Laplace Transform Theory* (Van Nostrand, London, 1966).